

Near-infrared laboratory spectra of H₂O trapped in N₂, CH₄, and CO: hints for trans-Neptunian objects' observations

D. Fulvio^{1,2}, S. Guglielmino², T. Favone², and M. E. Palumbo²

¹ Dipartimento di Fisica e Astronomia, Università di Catania, via Santa Sofia 64, 95123 Catania, Italy
e-mail: dfu@oact.inaf.it

² INAF – Osservatorio Astrofisico di Catania, via Santa Sofia 78, 95123 Catania, Italy
e-mail: mepalumbo@oact.inaf.it

Received 14 July 2009 / Accepted 16 November 2009

ABSTRACT

Context. Recent mid-infrared spectroscopic observations of Pluto and Triton suggest a wide distribution of H₂O ice into surface regions containing more volatile species such as N₂, CH₄, and CO. This disagrees with the common idea that because of their typical surface temperature, water should not be involved in volatile transport processes, standing easily segregated from the more volatile species.

Aims. We analyse infrared H₂O band profiles when water is diluted in solid matrices dominated by methane, carbon monoxide, and/or molecular nitrogen. We also show the results of temperature-related diffusion processes of solid N₂ into H₂O ice deposited at different temperatures. Finally, we analyse ion irradiation effects for some of the mixtures considered.

Methods. Solid samples were analysed by infrared (1.0–16.0 μm) transmission and reflectance spectroscopy at different temperatures (15–150 K), before and after ion irradiation with 200 keV protons.

Results. When water is highly diluted in solid matrices, the profile of its near-infrared bands is strongly modified. Two narrow bands appear around 1.89 μm and 1.39 μm instead of the well known pure water ice bands at 2 μm and 1.5 μm, respectively. Furthermore, the peak position and width of the 1.89 and 1.39 μm bands depend on the initial mixture water is embedded in. The intensity of these bands decreases after ion irradiation.

Conclusions. Since the mixtures considered closely resemble the surface composition of trans-Neptunian objects, experiments here discussed show that the bands around 1.89 μm and 1.39 μm are appropriate to investigating the presence of diluted water regions on their surface. In fact, the irradiation dose required for a significant decrease in their intensity would be accumulated on a timescale larger than the timescale for resurfacing processes on the surfaces of trans-Neptunian objects. Results shown here will contribute in a strong way to the interpretation of New Horizons near-infrared observations.

Key words. Kuiper belt: general – methods: laboratory – techniques: spectroscopic – infrared: planetary systems – line: profiles – molecular processes

1. Introduction

In the outer Solar System, beyond Neptune's orbit, there is a population of small bodies collectively named trans-Neptunian objects (TNOs) (see e.g., Barucci et al. 2008; Gladman et al. 2008). Interest in these bodies is justified because they are considered to be the memory of the origin and evolution of the early Solar System (e.g. Jewitt and Luu 1993; Luu et al. 1997).

So far, about 40 TNOs have been observed in the near-infrared spectral range and we can distinguish among three main classes of TNO surface compositions. The first one is constituted by TNOs whose spectra are dominated by methane-ice absorption bands, such as Pluto (Owen et al. 1993; Protopapa et al. 2008), Eris (Brown et al. 2005; Licandro et al. 2006b; Dumas et al. 2007), and Makemake (Licandro et al. 2006a; Brown et al. 2007; Tegler et al. 2007; Tegler et al. 2008). A similar spectrum is also shown by Triton (Cruikshank et al. 1993, 2000; Quirico et al. 1999), probably an originally isolated TNO that was then captured by Neptune (McKinnon et al. 1995). The second class is constituted by TNOs with water-ice dominated spectra, such as (13308) 1996 TO66 (Brown et al. 1999), Varuna (Licandro et al. 2001), and Haumea (Pinilla-Alonso et al. 2009). The third class contains TNOs whose spectra are featureless (see for

instance Doressoundiram et al. 2003; and Barkume et al. 2008). In fact, this is just a general classification, since some TNOs show both methane and water-ice absorption bands, such as Sedna (Barucci et al. 2005) and Quaoar (Jewitt & Luu 2004; Shaller & Brown 2007).

Laboratory experiments discussed here refer to the first class of TNOs whose infrared spectra clearly show methane-ice features. In addition to the CH₄ absorption bands, these spectra can also show additional near-infrared features from solid H₂O, CO₂, and more volatile species, such as N₂ and CO.

For instance, Pluto's near-infrared spectra clearly show all those features but CO₂ (Owen et al. 1993; Douté et al. 1999; Young et al. 2008). So far, the most credited model of Pluto surface admits three distinct surface units (Douté et al. 1999; Lellouch et al. 2000; Grundy & Buie 2001; Olkin et al. 2007). The first one has either a N₂-rich terrain with traces (less than 1% by volume) of CO and CH₄ or a thin layer of pure fine-grained CH₄ covering a compact mixture of N₂ (about 99% by volume): CO (0.1–0.2%): CH₄ (about 0.5%); the second unit includes pure large-grained CH₄ or a N₂: CO: CH₄ mixture covering a substrate of pure large-grained CH₄. The last unit is constituted by fine-grained pure N₂ or by a mixture of water ice and tholin-type radiolysis/photolysis residues. In a similar way, the most

credited surface model of Triton admits two possible scenarios (Quirico et al. 1999; Cruikshank et al. 2000). Both the possibilities present a common N₂-dominant region with traces of CO and CH₄ and, for the remaining surface unit, the first scenario admits a region made of an H₂O: CO₂ mixture, while in the second scenario water ice and carbon dioxide are geographically separated.

Since solid N₂, CH₄, and CO are more volatile than water and, keeping in mind that the typical TNO's surface temperature is lower than 50 K, the common idea is that on TNOs' surfaces water should not be involved in volatile transport processes and, for this reason, it should stand easily segregated from former species. Despite that, recent infrared spectroscopic observations of Pluto and Triton give a clue to the wide surface distribution of H₂O ice in those regions containing more volatile N₂ and CH₄ species (Grundy et al. 2002; Grundy & Buie 2002). Thus it cannot be excluded that a small quantity of water molecules is trapped in a volatile matrix on TNOs' surfaces.

Several laboratory studies have shown that, when water is diluted in solid matrices, very sharp discrete bands appear (Tursi & Nixon 1970; Ayers & Pullin 1976a,b; Nelander, 1988; Ehrenfreund et al. 1996; Satorre et al. 2001; Palumbo & Strazzulla 2003). In particular, Satorre et al. (2001) have shown that, when water is highly diluted in a nitrogen matrix, the broad absorption band of pure water ice around 2.0 μm becomes a narrow feature at about 1.89 μm suggesting us that under some conditions we have to move the search for near-infrared water ice spectral features toward different wavelengths.

In this work we want to extend the experimental results obtained by Satorre et al. (2001) to different binary and ternary mixtures of CH₄, CO, N₂, and H₂O closely resembling the surface composition of the considered class of TNOs. We show that the profile of both the 2.0 μm and 1.5 μm water bands is strongly modified when water is highly diluted in ice matrices. Thanks to these results we show the importance of the 1.89 μm and 1.39 μm isolated water-ice features as a diagnostic probe for searching regions on planetary surfaces where water could be diluted in other dominant species.

Finally, we show the spectral changes induced on the profile of the 1.89 μm band by solar wind ion and cosmic-ray bombardment suffered by these objects. To do this we performed different ion irradiation experiments to simulate the irradiation conditions in the outer Solar System. Results shown here will be discussed in the light of the NASA New Horizons mission (launched in 2006) to Pluto-Charon system.

2. Experimental setup

Experiments discussed here were performed in the Laboratory for Experimental Astrophysics at INAF – Osservatorio Astrofisico di Catania (Italy). The experimental apparatus used to obtain infrared transmittance and reflectance spectra of the considered icy samples in the range 10 000–600 cm⁻¹ (1.0–16.0 μm) is composed of a stainless steel high-vacuum chamber operating at a pressure $P < 10^{-7}$ mbar facing an FTIR spectrophotometer (Bruker Vertex 70 or Bruker Equinox 55) through KBr windows. Inside the vacuum chamber, frozen species are accreted onto the substrate to operate in reflectance or transmittance configuration. In reflectance configuration, a gold substrate is used, while in transmittance configuration the substrate is an infrared transparent material such as crystalline Si or KBr. In both cases the substrate is placed in thermal contact with a closed-cycle helium cryostat whose temperature can be varied

between 10 and 300 K. A detailed depiction of the discussed set-up can be found in Brunetto & Strazzulla (2005, Fig. 1).

Gas mixtures are prepared (in the chosen relative ratio) in a mixing chamber and admitted into the high-vacuum chamber by means of a gas inlet. With our experimental set-up, we can monitor the thickness of the ice film during its accretion by looking at the interference pattern (intensity versus time) given by an He – Ne laser beam (543 nm) reflected, at both 2.9° (Fulvio et al. 2009) or 45° (Baratta & Palumbo 1998) incidence, by the vacuum – film and film – substrate interfaces.

The vacuum chamber is interfaced with an ion implanter (Danfysik) from which ions with energy up to 200 keV (400 keV for double ionization) can be obtained. The ion beam generated by the implanter is swept to produce, on the target, a spot greater than the area probed by the infrared beam. The current intensity is kept below few tenths of μA cm⁻², in order to avoid a macroscopic heating of the sample. To compare results obtained after irradiation of different targets, the ion fluence (ions/cm²) is converted to dose (eV/16 u; u = unified atomic mass unit).

The substrate is mounted at an angle of 45° with respect to both the ion beam and the infrared beam. For this reason spectra can be acquired “in-situ” before and after irradiation, without tilting or rotating the sample. Sample temperature can be managed by means of a resistance heater directly connected to the cryostat so that spectra can be easily taken at selected temperature in the range 10–300 K.

All the ion irradiation experiments were performed by irradiating samples with thickness (typically less than 1 μm) lower than the penetration depth of the considered ions to uniformly irradiate the sample. On the other hand, in the case of experiments devoted to studying the changes in water band profile arising when water is diluted in binary and ternary solid matrices, we deposited thicker samples (between 5 and 60 μm) to be able to study weak spectral features. For each considered mixture, two spectra were recorded, one with the electric vector parallel (P polarized) and one perpendicular (S polarized) to the plane of incidence. The polarization was selected using a rotatable polarizer placed in the path of the infrared beam.

It has been shown (Baratta et al. 2000; Palumbo et al. 2006) that if the transitions are “strong” then the band profiles recorded in P and S polarization are different. On the other hand, when the transitions are “weak” the band profiles recorded in P and S polarization are similar, and the features seen in the transmission spectra directly reflect variations in the absorption coefficient of the solid sample. The latter circumstance has been observed for the bands discussed in the following so we will show the P polarized spectra, since the signal-to-noise ratio is higher for this polarization.

All the transmittance spectra were recorded with a resolution of 1–2 cm⁻¹. Reflectance spectra were recorded with a resolution of 8 cm⁻¹ to improve the signal-to-noise ratio. At the beginning of each experiment, after the substrate reached the selected temperature, two background spectra (P and S polarization) were acquired. Spectra taken after sample deposition (or after each step of irradiation) were referred to the background spectrum recorded at the corresponding polarization.

We want point out that transmittance spectra were obtained with respect to the bare substrate. Because of interference effects (coating) the resulting transmittance of the coated substrate, in a non-absorbing spectral region, can be greater (depending on the thickness of the ice film and on the wavelength) than the transmittance of the uncoated substrate (i.e., the film behaves as an anti-reflection coating) giving a transmittance value greater than one (Macleod 1986; Palumbo et al. 2006). In the case of

reflectance spectra, the substrate used is the gold coating of a quartz micro-balance that is not optically flat. Indeed the light is collected at 45° off the specular direction. In these experimental conditions, the ice film causes an increase of the diffused light, explaining why the reflectance value is greater than one in the reflectance spectra shown in this paper.

More details on the experimental apparatus and procedures can be found in Baratta & Palumbo (1998), Palumbo et al. (2004), Brunetto & Strazzulla (2005), and Fulvio et al. (2009).

3. Results

Water-ice morphology/structure strongly depends on deposition conditions such as temperature, deposition rate, and growth angle (e.g., Hagen et al. 1983; Jenniskens & Blake 1994; Westley et al. 1998; Kimmel et al. 2001a,b; Dohnálek et al. 2003).

It is well known (see, for instance, Hudgins et al. 1993; Quirico et al. 1999; Gerakines et al. 2005; Mastrapa et al. 2008) that the infrared spectrum of amorphous solid water (i.e., deposition temperature lower than 100 K), in the range 10 000–600 cm⁻¹ (1.0–16.0 μm), shows absorption bands at about 6660 cm⁻¹ (1.5 μm; overtone and combination of symmetric and anti-symmetric stretching modes), 5000 cm⁻¹ (2 μm; combination of bending and stretching modes), 3300 cm⁻¹ (3.03 μm; O-H symmetric and anti-symmetric stretching modes), 2205 cm⁻¹ (4.53 μm; combination mode), 1650 cm⁻¹ (6.06 μm; overtone of the libration mode and bending mode), and 803 cm⁻¹ (12.4 μm; libration mode). Two small features are also present on the wing of the O-H stretching modes band, whose peak positions are at 3720 and 3697 cm⁻¹ (2.69 and 2.70 μm, respectively). These weak bands come from O-H dangling bonds in the micropores of the porous structure of amorphous water ice (e.g., Rowland et al. 1991; Palumbo 2006). By warming up amorphous water-ice, a more ordered (i.e. crystalline) structure is obtained as a function of the increasing temperature, and the profile of H₂O bands is deeply modified. Water-ice morphology also changes under ion/photon irradiation. Indeed it has been shown that crystalline water ice is converted to amorphous ice by irradiation (Baratta et al. 1991; Moore & Hudson 1992; Leto & Baratta 2003) and that the porosity of amorphous water ice decreases after ion irradiation (Palumbo 2006; Raut et al. 2008).

In the following sections we show the results concerning infrared spectral features appearing in different binary and ternary mixtures of CH₄, CO, N₂, and H₂O (Sect. 3.1); temperature-related diffusion processes of solid N₂ in H₂O ice at different temperatures (Sect. 3.2); and ion irradiation experiments on N₂:H₂O mixtures (Sect. 3.3).

3.1. Binary and ternary mixtures

In Fig. 1 we show the reflectance spectrum of amorphous solid water as deposited at 16 K in the spectral region of our interest (7500–4500 cm⁻¹). Figure 2 shows in two spectral regions the NIR spectra of CH₄:H₂O = 100:1 and CO:H₂O = 100:1 mixtures at 16 K. The spectrum of the N₂:H₂O = 100:1 mixture, adapted from Satorre et al. (2001), is also shown for comparison. The panels on the righthand side show that the band at around 5300 cm⁻¹ (1.89 μm) is present in all of these mixtures. The third panel (top to bottom) shows the spectrum of the N₂:H₂O = 100:1 mixture at 15 K recorded in reflectance mode. We notice that, in the case of N₂:H₂O samples, the 5300 cm⁻¹ band is present in both spectra recorded in transmittance or reflectance mode with the same peak position. On the other hand,

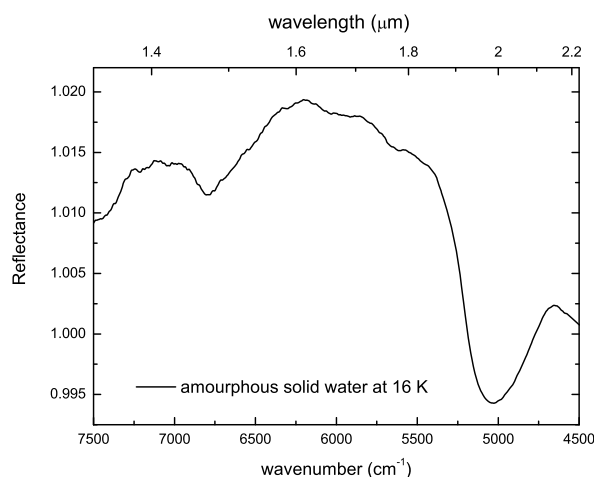


Fig. 1. Reflectance spectrum of amorphous solid water at 16 K in the spectral range 7500–4500 cm⁻¹.

the different width of the band profiles stems from the different spectral resolutions. Furthermore, the profile of the 5300 cm⁻¹ band is the same when the spectrum is recorded in S or P polarization (see Sect. 2); then, our laboratory spectra, both in reflectance and transmittance, can be compared (e.g., band position, band shape) with the reflectance spectra of Solar System objects (Baratta et al. 2000; Palumbo et al. 2006).

Among the transmittance spectra shown, the 5300 cm⁻¹ band profile in the case of the CH₄:H₂O mixture looks broader than the case of CO:H₂O and N₂:H₂O mixtures. Band peak is centered at 5289, 5292, and 5303 cm⁻¹ for CO:H₂O, CH₄:H₂O and N₂:H₂O mixture (see Table 1), respectively, indicating that its position depends on the dominant species in which water is trapped. Moreover, in the case of the CH₄:H₂O mixture, the band visible at 5384 cm⁻¹ comes from CH₄ (Quirico & Schmitt 1997).

In the lefthand side of Fig. 2 we show the spectral feature arising around 7180 cm⁻¹ when water is isolated in the considered binary mixtures. This band is evident at 7199 cm⁻¹ in the reflectance spectrum of N₂:H₂O = 100:1 mixture. For this mixture we do not show the transmittance spectrum because of its low signal-to-noise ratio. For the CO:H₂O = 100:1 mixture, we can see the same spectral feature whose peak position is at 7160 cm⁻¹. Due to a little change in the background occurring during the spectral acquisitions, this spectrum presents some background features pointing in the opposite direction from the absorption bands. In the case of the CH₄:H₂O = 100:1 mixture, we can see all the main absorption bands of CH₄ in the spectral range 10 000–3000 cm⁻¹ (Quirico & Schmitt 1997 and references therein). In particular, on the lefthand side of Fig. 2, we are able to identify the CH₄ band at 7130 cm⁻¹. In this figure we can also see two absorption bands at 7276 and at about 7181 cm⁻¹. We think that the feature at about 7181 cm⁻¹ corresponds to those seen in both binary mixtures N₂:H₂O and CO:H₂O (at 7199 and 7160 cm⁻¹, respectively), and its peak position is shifted because of the particular mixture considered. In fact, CH₄ has two additional weak bands in the spectral region shown in Fig. 2, but their peak position (7233 and 7193 cm⁻¹) differs from that of the bands seen here. Further experimental work is required to identify the feature appearing at 7276 cm⁻¹ (1.37 μm).

Figure 3 shows the NIR spectra of different N₂:CH₄:H₂O ternary mixtures at 12 K. The 1.89 μm band is present in all

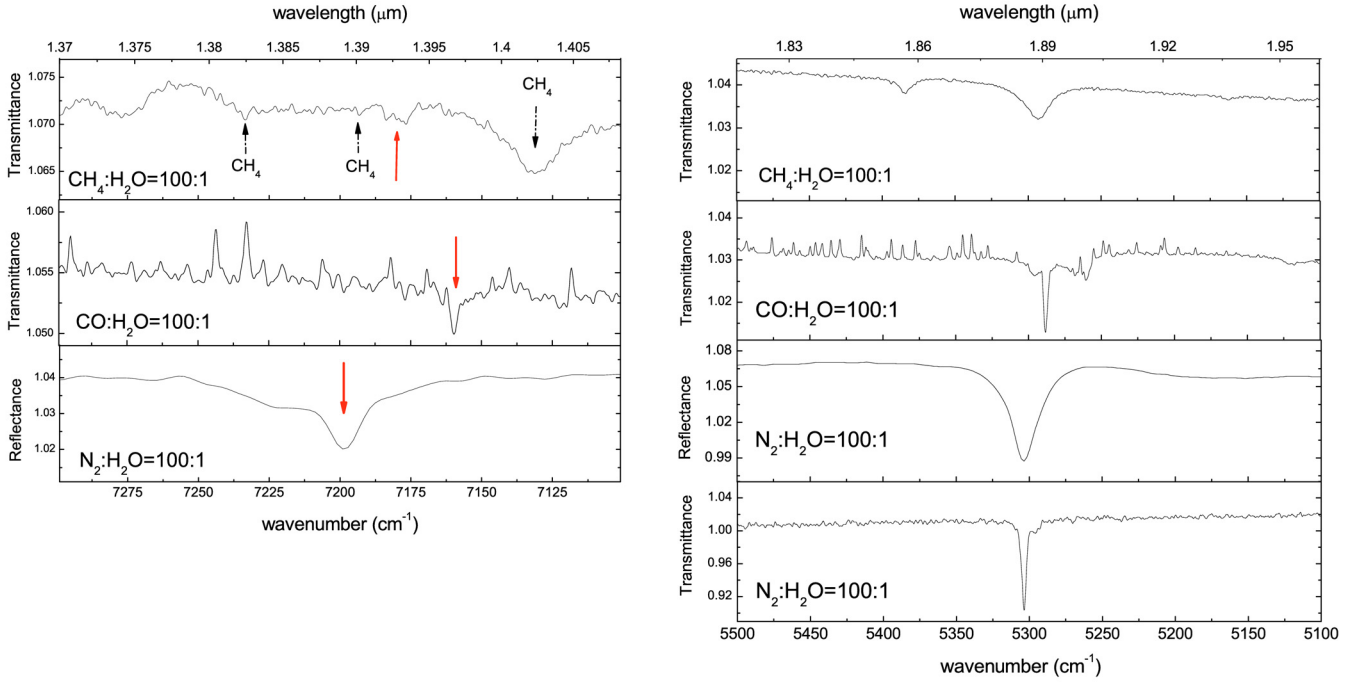


Fig. 2. Spectra of $\text{CH}_4:\text{H}_2\text{O} = 100:1$, $\text{CO}:\text{H}_2\text{O} = 100:1$ and $\text{N}_2:\text{H}_2\text{O} = 100:1$ mixtures at 16 K in two different spectral ranges: $5500\text{--}5100\text{ cm}^{-1}$ (righthand side) and $7300\text{--}7100\text{ cm}^{-1}$ (lefthand side). In the latter case solid arrows help the reader to clearly identify the bands arising when water is isolated in the considered matrix. Dotted arrows refer to the position of the known CH_4 bands at 7233 , 7193 and 7130 cm^{-1} . For the mixture $\text{N}_2:\text{H}_2\text{O}$ we have not shown the transmittance spectrum in the $7300\text{--}7100\text{ cm}^{-1}$ range because of its low signal to noise ratio.

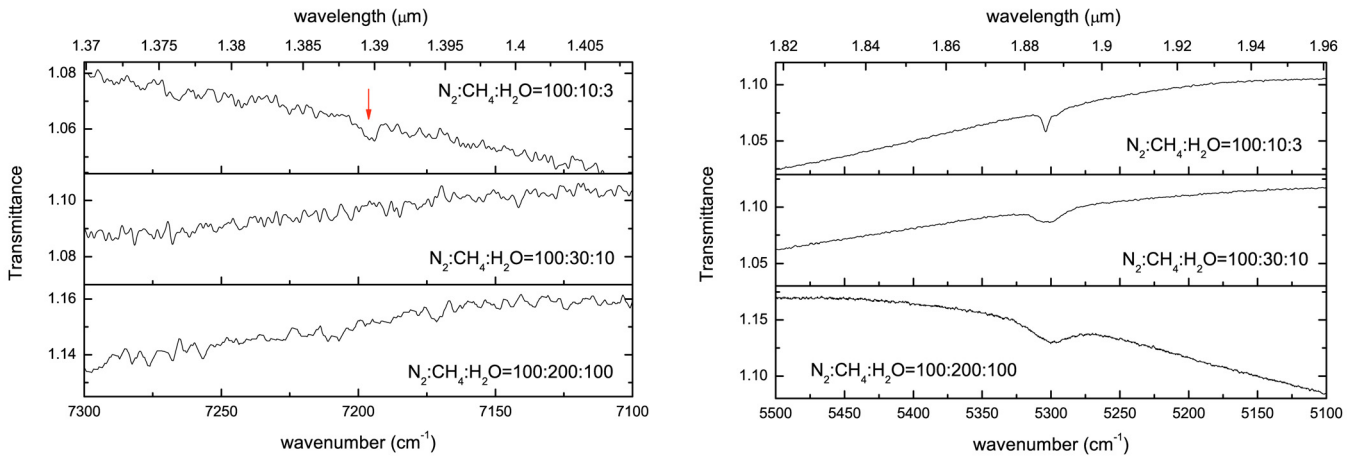


Fig. 3. Ternary mixtures of $\text{N}_2:\text{H}_2\text{O}:\text{CH}_4$ at 12 K with different relative amounts of N_2 , H_2O , and CH_4 . Same spectral ranges as Fig. 2. Solid arrow points at the band arising at 7195 cm^{-1} when water is isolated in N_2 -dominated solid matrix. Spectra shown in the righthand side are adapted from Satorre et al. (2001).

Table 1. Peak position and relative intensity of the band around 7180 cm^{-1} (referred to as BII) with respect to the band around 5300 cm^{-1} (referred to as BI).

Mixture	BI peak position (cm^{-1})	BII peak position (cm^{-1})	BII/BI
$\text{CH}_4:\text{H}_2\text{O} = 100:1$	5292	7181	0.24 ± 0.04
$\text{CO}:\text{H}_2\text{O} = 100:1$	5289	7160	0.22 ± 0.06
$\text{N}_2:\text{H}_2\text{O} = 100:1$	5303	7199	0.24 ± 0.03
$\text{N}_2:\text{CH}_4:\text{H}_2\text{O} = 100:10:3$	5303	7195	0.30 ± 0.09
$\text{N}_2:\text{CH}_4:\text{H}_2\text{O} = 100:30:10$	5302	–	–
$\text{N}_2:\text{CH}_4:\text{H}_2\text{O} = 100:200:100$	5300	–	–

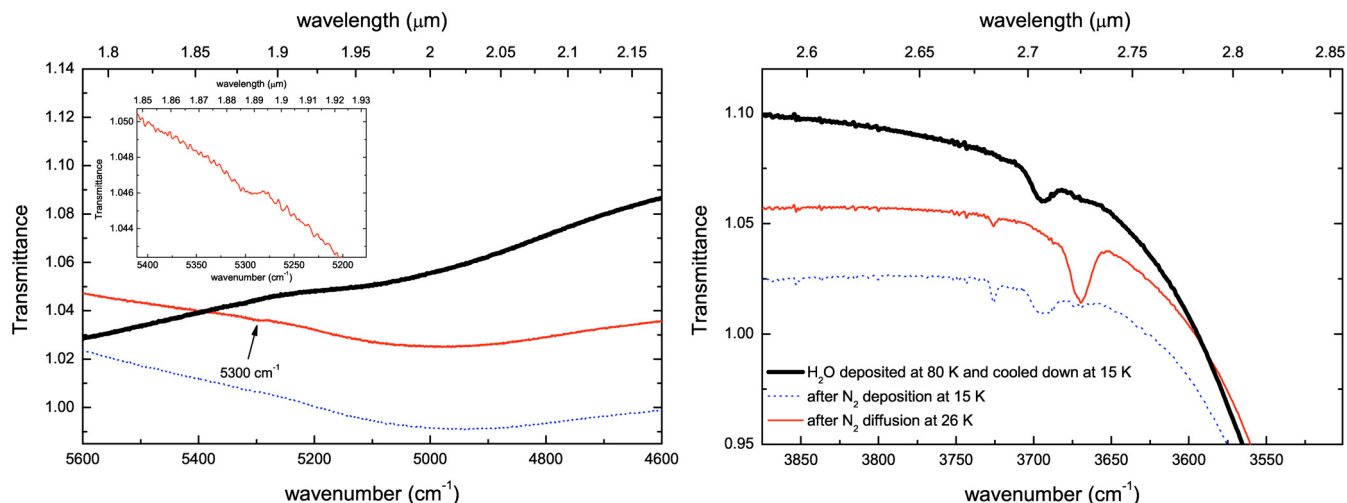


Fig. 4. Diffusion of N₂ deposited at 15 K on water ice deposited at 80 K and cooled down at 15 K. Two different spectral regions are considered.

spectra shown, while we only observe the 1.39 μm band in the N₂:CH₄:H₂O = 100:10:3 mixture (that is, the mixture with the lowest H₂O relative abundance). Its band peak position is at 7195 cm⁻¹ (see again Table 1). Concerning its intensity, we can exclude any contribution from the CH₄ band at 7193 cm⁻¹ (see Fig. 2). In fact CH₄ shows a stronger band at 7130 cm⁻¹ (Quirico & Schmitt 1997), which is not present in our spectrum. For the two other mixtures shown in Fig. 3, the signal-to-noise ratio reached in our experiments in the considered spectral region is not enough to be able to tell if any band is present, so further experimental work is required. From the CH₄ bands at 2818, 4204, and 4302 cm⁻¹, using the band strength values given by Brunetto et al. (2008), we estimated that the column density of CH₄ in the binary mixture CH₄:H₂O = 100:1 is about 7, 20, and 32 times higher than the CH₄ column density in the ternary mixture N₂:CH₄:H₂O = 100:200:100, 100:30:10, and 100:10:3, respectively. Then we do not expect to detect the 7130 cm⁻¹ CH₄ band in the spectra of the ternary mixtures.

It has been suggested (Satorre et al. 2001; Palumbo & Strazzulla 2003) that, when water is highly diluted in solid matrices, the profile of the 5000 cm⁻¹ (2 μm) band (see Fig. 1) is transformed into the narrow 5300 cm⁻¹ (1.89 μm) band. Similarly we now suggest that the profile of the broad 6650 cm⁻¹ (1.5 μm) band (see again Fig. 1) is transformed into the narrow band at around 7180 cm⁻¹ (1.39 μm).

For all the mixtures considered where both bands at about 5300 and 7180 cm⁻¹ are present, we also calculated the relative intensity on optical depth scale of the band at around 7180 cm⁻¹ with respect to the band at around 5300 cm⁻¹. These values and their error bars (which depend on the noise of each spectrum) are reported in Table 1.

3.2. Diffusion of N₂ in H₂O

When N₂ is deposited on amorphous solid water, a layered sample is obtained (i.e., Palumbo 2006). If this sample is warmed up, at about 30 K, N₂ diffusion in the porous structure of solid water takes place. The diffusion is proven by the shift of the O-H dangling bonds features from 3697 to 3672 cm⁻¹ and from 3720 to 3690 cm⁻¹ (Rowland et al. 1991; Palumbo & Strazzulla 2003). Furthermore, Palumbo & Strazzulla (2003) have shown

that a band at 5300 cm⁻¹ appears after diffusion of N₂ in porous amorphous solid water.

To extend the results obtained by Palumbo & Strazzulla (2003), in this paper we considered two new cases: 1) N₂ condensed at 15 K on frozen water previously deposited at 80 K (i.e. an intermediate case between the amorphous and crystalline one) and 2) N₂ condensed at 15 K on water-ice previously deposited at 150 K (i.e., crystalline water ice). In both cases the obtained samples were afterwards warmed (26–32 K) to induce the diffusion of N₂ into H₂O. The diffusion was probed in both experiments by means of the narrow feature arising around 5300 cm⁻¹ and, in the case of water ice deposited at 80 K, also by means of the shift of the O-H dangling bond' peak position (Rowland et al. 1991; Palumbo & Strazzulla 2003).

Figure 4 shows, in two different spectral regions, the spectrum of N₂ condensed at 15 K on water ice previously deposited at 80 K and cooled down to 15 K. We can see the broad absorption band at about 5000 cm⁻¹ due to polymeric water. Moreover, as discussed by Rowland et al. (1991), the profile of the O-H dangling bond depends on the temperature of the sample; in particular, the spectrum of water ice cooled from 80 K to 15 K shows only the O-H dangling bond band at 3695 cm⁻¹, so we can use it, together with the 5300 cm⁻¹ band, to investigate if N₂ diffusion is occurring. After N₂ deposition at 15 K, we can see a change in the continuum trend around 5000 cm⁻¹ because of the increasing thickness of the deposited ice. This is proof that N₂ deposition took place. In the region 3900–3500 cm⁻¹ we see a weak band at 3725 cm⁻¹ due to a small amount of monomeric/dimeric H₂O co-deposited with N₂ at 15 K (Ehrenfreund et al. 1996). The icy sample so obtained was then sequentially warmed up, and at 26 K we observed diffusion of N₂ in H₂O ice. In fact, we can see in Fig. 4 the shift of the O-H dangling bond peak position from 3695 cm⁻¹ to 3670 cm⁻¹ and the appearance of the weak feature around 5300 cm⁻¹. These changes testify to the migration of N₂ molecules from the frozen overlay into water-ice layers (Palumbo & Strazzulla 2003), so the result of this experiment is that N₂ condensed at 15 K on water ice previously deposited at 80 K diffuses in H₂O when warming the sample at about 26 K. After diffusion a small feature at about 3725 cm⁻¹ is still present in the spectrum. This testifies that N₂ diffuses in the underneath porous ice sample but partially remains on its top.

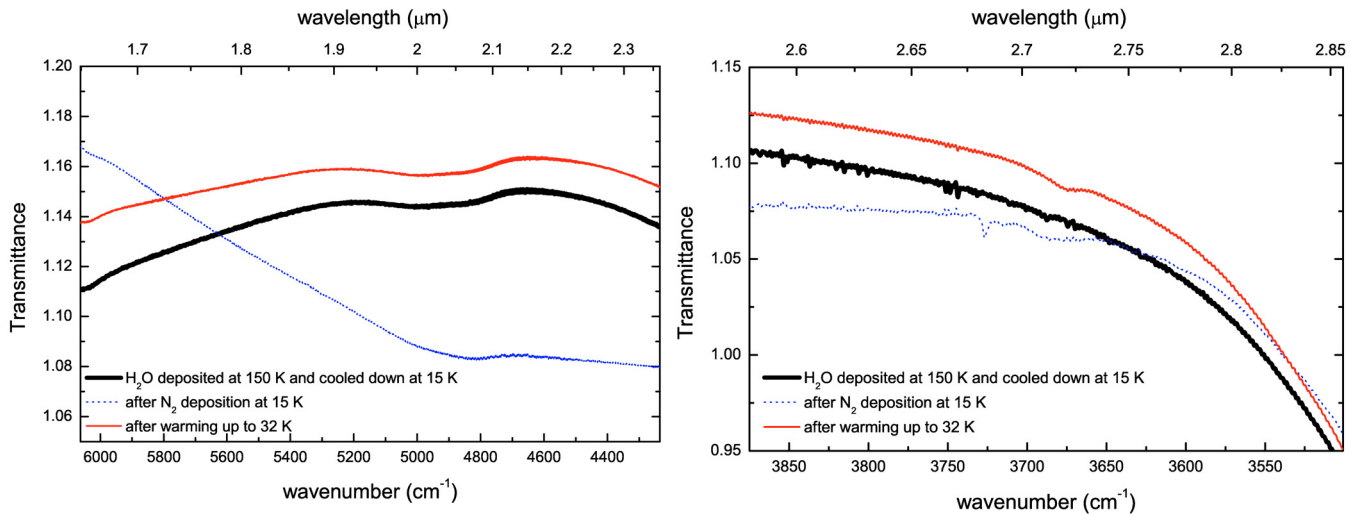


Fig. 5. Attempted diffusion of N_2 deposited at 15 K on crystalline water ice deposited at 150 K and cooled down at 15 K. Two different spectral regions are considered.

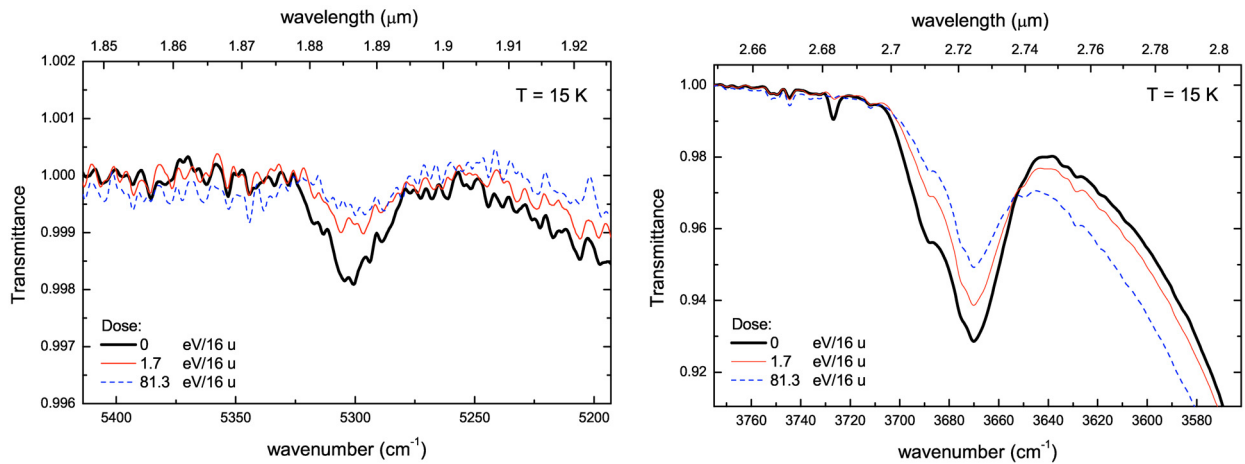


Fig. 6. Ion irradiation (with 200 keV H^+ ions) of an $H_2O:N_2$ mixture obtained after diffusion of N_2 into water ice previously deposited at 15 K. On the righthand side, destruction of the O-H dangling bonds features at 3672 and 3690 cm^{-1} is shown as a function of the increasing irradiation dose. On the lefthand side, destruction of the 5300 cm^{-1} feature is shown.

Figure 5 shows the spectrum of N_2 condensed at 15 K on water ice previously deposited at 150 K and cooled down to 15 K. In crystalline water-ice, O-H dangling bonds are present just at the surface of large ice clusters (Rowland et al. 1991), and the intensity of the related spectral features is too weak to be detected in our experimental conditions (Palumbo 1997), so we cannot use them to investigate whether N_2 diffusion is occurring. After N_2 deposition at 15 K, the change in the continuum trend comes from the increased thickness of the deposited ice. In the 3900–3500 cm^{-1} region shown in Fig. 5, after N_2 deposition, we see the rise of two weak bands at 3725 and 3685 cm^{-1} . As in the previous case (see Fig. 4), these bands come from a little residual amount of H_2O inside the vacuum chamber and co-deposited with N_2 at 15 K (Ehrenfreund et al. 1996). The icy sample so obtained was then warmed by increasing the temperature sequentially up to about 32 K in order to induce diffusion of N_2 in H_2O ice but, within our errors, there is no spectral evidence for it. In fact, up to 32 K we do not see the appearance of the narrow feature around 5300 cm^{-1} that would indicate the migration of N_2 molecules into the water ice, and at about 32 K, N_2 sublimates (Fig. 5). Thus this experiment shows that N_2

condensed at 15 K on water ice previously deposited at 150 K (i.e., crystalline water ice) does not diffuse when warming the sample.

3.3. Ion irradiation experiments

Effects of irradiation with 200 keV H^+ ions at different fluences on pure amorphous water ice (at 15 K) were discussed in Palumbo (2006), where it is shown that the band area of O-H dangling bonds (considering the summed area of both bands at 3697 and 3720 cm^{-1}) decreases as the total dose (see Sect. 2) increases. This effect stems from the destruction of O-H dangling groups in the micropores by ion irradiation, i.e. a modification of the physical structure of the sample (Palumbo 2006; Raut et al. 2008).

Figure 6 shows the effects of 200 keV H^+ ion irradiation in an $H_2O:N_2$ mixture obtained after diffusion of N_2 in water ice previously deposited at 15 K. Diffusion was obtained by warming the sample to about 30 K (see Palumbo & Strazzulla 2003), and the mixture so obtained was finally cooled down to 15 K. On the righthand side of Fig. 6, we can see that also in this case

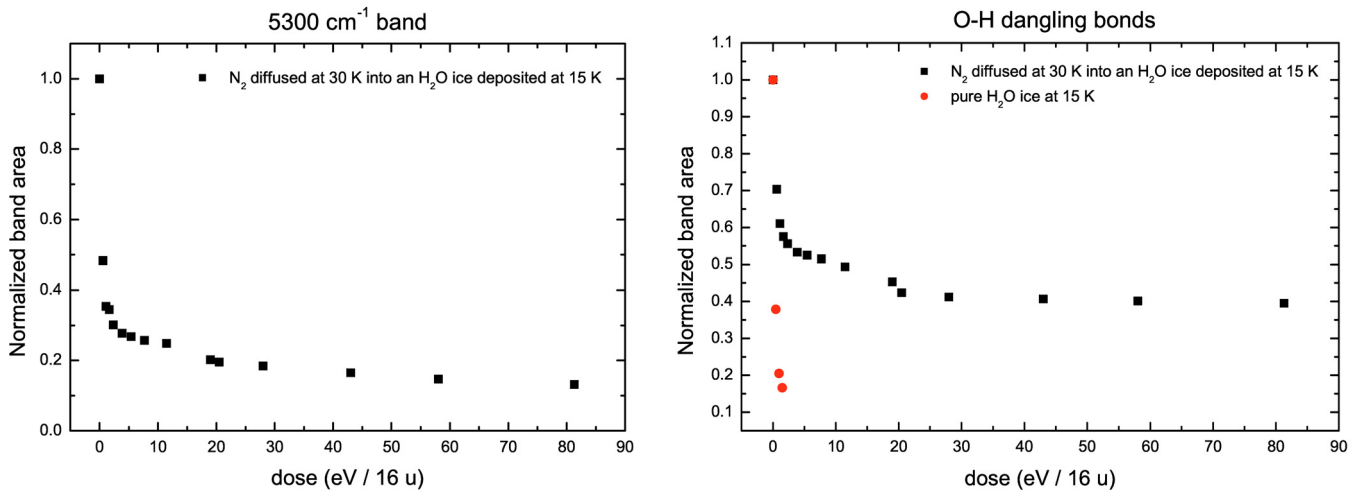


Fig. 7. Normalized integrated intensity of the O-H dangling bond (righthand side) and 5300 cm⁻¹ (lefthand side) features as a function of the increasing irradiation dose for a H₂O:N₂ mixture obtained after diffusion of N₂ into water ice previously deposited at 15 K. In the case of the O-H dangling bond feature the case of pure water ice at 15 K is also shown (values reported by Palumbo 2006). Band area values are normalized to the initial value.

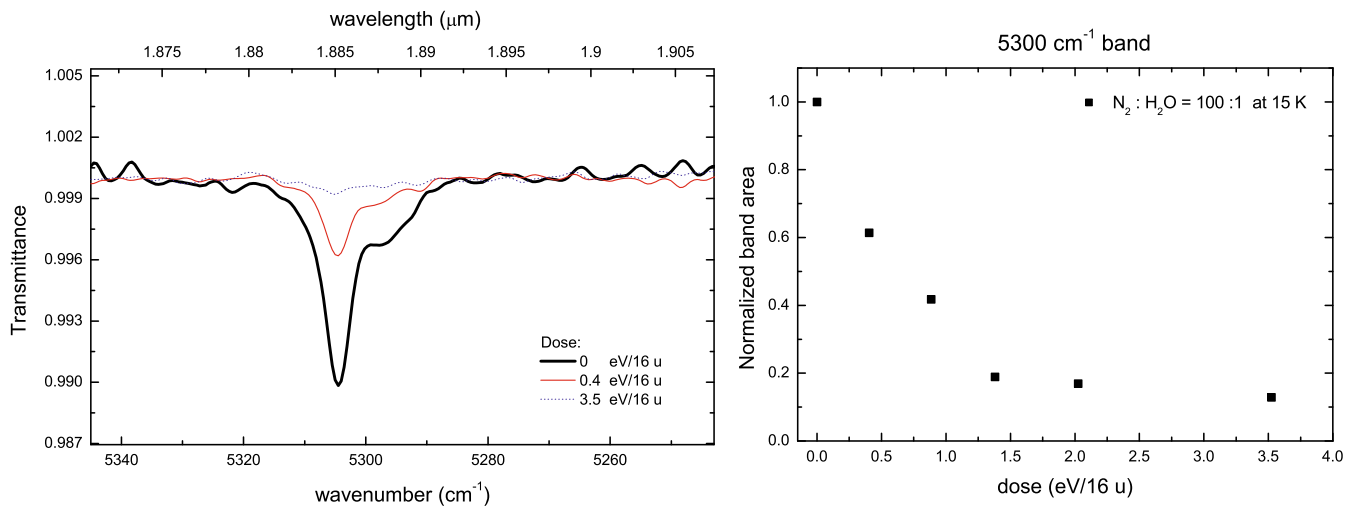


Fig. 8. Ion irradiation (200 keV H⁺ ions) of a N₂:H₂O = 100:1 mixture at 15 K. In the lefthand side, spectra before and after irradiation at different dose are shown. On the righthand side, destruction of the feature around 5300 cm⁻¹ is shown as a function of the increasing irradiation dose. Band area values are normalized to the initial value.

the band area of the O-H dangling bonds at 3670 and 3688 cm⁻¹ (different band shape and peak positions with respect to the case of pure water-ice come from the diffusion) decreases as the total dose increases, but now the destruction yield of the considered band area is lower than in the case of pure amorphous water ice at 15 K (Palumbo 2006). This behaviour is similar to the case of H₂O:X mixtures studied by Palumbo (2006). In fact, at the higher dose reached in our experiments (81.3 eV/16 u), the considered area is reduced to about 40% of the initial value (see Fig. 7).

On the lefthand side of Fig. 6, ion irradiation effects are also shown for the narrow spectral feature around 5300 cm⁻¹ (1.89 μm). This band is destroyed under irradiation and, at the higher dose reached in our experiments (81.3 eV/16 u), the value of its area is about 15% of the original one (see Fig. 7).

Figure 8 shows the results obtained after ion irradiation with 200 keV H⁺ of a N₂:H₂O = 100:1 mixture. The intensity of the 5300 cm⁻¹ band decreases as the irradiation dose increases, and

the value of its area is about 15% of the original one after a dose of 3.5 eV/16 u. The band area values shown in Figs. 7 and 8 have been measured after converting the spectra from transmittance to optical depth scale.

4. Discussion and conclusions

Results presented in this paper suggest that we look for the bands at 1.89 μm (~5300 cm⁻¹) and 1.39 μm (~7180 cm⁻¹) to investigate the regions on planetary surfaces of outer Solar System objects where water ice could be diluted in some dominant volatile species. All the species considered in this work (i.e. N₂, CH₄, and CO) are more volatile than water, so we expect that at TNO surface temperature (typically less than 50 K), water is not involved in volatile transport processes, standing easily segregated from them. Despite that, we cannot exclude a priori finding, on these objects, some surface regions where water is highly diluted in them. For example this could be the case occurring on Pluto

and Triton surfaces, for which recent spectroscopic observations in the infrared range give a hint of the wide surface distribution of H₂O ice into those regions containing more volatile N₂ and CH₄ species (Grundy et al. 2002; Grundy & Buie 2002).

Explanation that justifies how H₂O ice could be present in regions dominated by volatile species is not fully understood, but different hypotheses appear plausible. It could be because of a co-deposition of the more volatile species, together with a small amount of water vapor escaped from the surface and trapped in the (tenuous, if any) atmosphere of such bodies or because of seasonal re-condensation processes of the more volatile species on water-rich surface regions with succeeding diffusion of N₂ in the underlying H₂O substrate as shown to occur in our experiments.

It is generally accepted that surfaces of airless bodies in the Solar System are continuously bombarded by energetic particles, such as solar wind ions and cosmic rays (Johnson 1990; Strazzulla & Johnson 1991; Strazzulla et al. 2003). The experimental results presented here show that the intensity of the 1.89 μm band decreases after ion irradiation. Then it is important to compare the dose range investigated in the laboratory with the irradiation doses suffered by TNOs to understand if it is reasonable to expect seeing this feature on their surfaces even after ion irradiation.

Estimation of the timescale of surface damage induced by ion irradiation in the outer region of the Solar System is difficult because of the sparse amount of data available about flux of energetic particles in those regions. Nevertheless, it is known that the main contribution to this flux is given by solar energetic particles and galactic cosmic-ray ions. It has been estimated that at ~ 40 AU an irradiation dose of 100 eV/16 u is reached, up to surface depths ~ 1 cm, on timescales of about 10^{10} years (see Strazzulla et al. 2003 and Cooper et al. 2003), i.e. 3.5 eV/16 u are reached in about 3.5×10^8 years. In the case of Pluto, since its orbital period is equal to about 2.5×10^2 years, its surface will experience this irradiation dose after $\sim 10^6$ orbits.

Experimental results presented in this paper indicate that the timescale for irradiation damage to the isolated water ice band at 1.89 μm is very long ($\sim 10^8$ years) compared to the timescale of seasonal re-surfacing processes (e.g., sublimations, condensations, metamorphism) occurring on TNOs' surfaces ($\sim 10^2$ – 10^3 years). Thus, the isolated water ice bands can appear in the near-IR spectra much more quickly than they can be destroyed by irradiation, and they therefore should be found in the spectra of methane/nitrogen-rich icy bodies in the outer Solar System.

Following this thought, we want to point out that there are some near-infrared spectra of TNOs showing a band (not yet identified) around 1.89 μm . In detail, the spectrum of Pluto published by Douté et al. (1999, Fig. 5) shows an unidentified band on the righthand side of the CH₄ band at 1.854 μm (same spectrum shown in Young et al. 2008); in the same way, Cruikshank et al. (2000) show this band in Fig. 1 in two spectra of Triton recorded on 1995 (the band on the righthand side in the triplet around 1.86 μm) and 1998 (the first visible band starting from 1.87 μm). The same unidentified band could be present, like a weak shoulder of the more prominent CH₄ feature, in Makemake's low-resolution spectra shown by Brown et al. (2007) and Licandro et al. (2006a).

All the spectra mentioned where a band around 1.89 μm is clearly visible are obtained by ground-based observations, so we have to take into account the data reduction problems arising because of the telluric atmospheric water vapor absorptions in the near-infrared regions around the considered bands

at 1.89 and 1.39 μm . In fact, there are a number of Pluto's spectra acquired outside the terrestrial atmosphere by the Hubble Space Telescope (HST), but their spectral resolution is too low to search for the band centred on 1.89 μm (Dumas et al. 2001; Grundy & Buie 2002). As an example, in Fig. 3 in Grundy & Buie (2002), ground-based Pluto's spectra obtained at high spectral resolution are re-sampled at the spectral resolution of HST/NICMOS. Although the high resolution spectra show the 1.89 μm band, when these spectra are re-sampled, the considered band disappears and we lose all information about it.

As far as we know, there are no available HST/NICMOS spectra with the spectral resolution ($R > 200$) required to search for that band. Nevertheless in 2006 NASA launched the New Horizons mission to Pluto-Charon system (encounter will be in 2015). The Ralph/LEISA instrument onboard New Horizons will obtain spectra in the 1.25 to 2.5 μm spectral region with an average spectral resolution $R = 240$ (Reuter et al. 2008), so the spectrometers onboard New Horizons mission will be able to search for the 1.39 and 1.89 μm bands. One of the main scientific goals of the New Horizons mission is to determine, via infrared observations, the surface distribution of solid N₂, CH₄, H₂O, and CO and to allow us a more sensitive search for additional surface species. Moreover, fulfilling as many of the Pluto-Charon scientific goals as possible, an extension of the mission will be devoted to at least another TNO.

In this work we have shown that the profile of both the 2.0 μm and 1.5 μm pure water bands is strongly modified when water is highly diluted in solid matrices. Two narrow bands appear around 1.89 and 1.39 μm instead of the pure water-ice bands. Moreover, we showed that diffusion of solid N₂ into H₂O ice is strongly dependent on the structure (amorphous vs. crystalline) of the H₂O ice. We performed different ion irradiation experiments to simulate the spectral changes induced on the profile of the 1.89 μm band by solar wind ions and cosmic-ray bombardment suffered by icy bodies in the outer Solar System. The irradiation dose required for a substantial decrease in the band intensity would be accumulated on a larger timescale than for re-surfacing processes on those icy objects. Our results show that the 1.89 and 1.39 μm isolated water-ice features are appropriate as diagnostic probes of regions on icy surfaces where water could be diluted in other dominant species. We think that the results shown here will contribute to interpret the New Horizons near-infrared observations.

Acknowledgements. We thank F. Spinella for his help on the experiments, and G. Strazzulla, G. A. Baratta, and R. Brunetto for their useful suggestions during this work. We acknowledge the financial support by Italian Space Agency, contract n. I/015/07/0 (Studi di Esplorazione del Sistema Solare).

References

- Ayers, G. P., & Pullin, A. D. E. 1976a, *Spectrochim. Acta*, 32A, 1629
- Ayers, G. P., & Pullin, A. D. E. 1976b, *Spectrochim. Acta*, 32A, 1695
- Baratta, G. A., & Palumbo, M. E. 1998, *J. Opt. Soc. Am. A*, 15, 3076
- Baratta, G. A., Leto, G., Spinella, F., Strazzulla, G., & Foti, G. 1991, *A&A*, 252, 421
- Baratta, G. A., Palumbo, M. E., & Strazzulla, G. 2000, *A&A*, 357, 1045
- Barkume, K. M., Brown, M. E., & Schaller E. L. 2008, *AJ*, 135, 55
- Barucci, M. A., Cruikshank, D. P., Dotto, E., et al. 2005 *A&A*, 439, L1
- Barucci, M. A., Boehnhardt, H., Cruikshank, D. P., & Morbidelli A. 2008, in *The Solar System Beyond Neptune* (Tucson: University of Arizona Press), 3
- Brown, R. H., Cruikshank, D. P., & Pendleton, Y. 1999, *ApJ*, 519, L101
- Brown, M. E., Trujillo, C. A., & Rabinowitz, D. L. 2005 *ApJ*, 635, L97
- Brown, M. E., Barkume, K. M., Blake, G. A., et al. 2007, *AJ*, 133, 284
- Brunetto, R., & Strazzulla, G. 2005, *Icarus*, 179, 265
- Brunetto, R., Caniglia, G., Baratta, G. A., & Palumbo, M. E. 2008, *ApJ*, 686, 1480

- Cooper, J. F., Christian, E. R., Richardos, J. D., & Wang, C. 2003, *Earth, Moon and Planets*, 92, 261
- Cruikshank, D. P., Roush, T. L., Owen, T. C., et al. 1993, *Science*, 261, 742
- Cruikshank, D. P., Schmitt, B., Roush, T. L., et al. 2000, *Icarus*, 147, 309
- Dohnálek, Z., Kimmel, G. A., Ayotte, P., Smith, R. S., & Kay, B. D. 2003, *J. Chem. Phys.*, 118, 364
- Doressoundiram, A., Tozzi, G. P., Barucci, M. A., et al. 2003, *AJ*, 125, 2721
- Douté, S., Schmitt, B., Quirico, E., et al. 1999, *Icarus*, 142, 421
- Dumas, C., Terrile, R. J., Brown, R. H., Schneider, G., & Smith, B. A. 2001 *AJ*, 121, 1163
- Dumas, C., Merlin, F., Barucci, M. A., et al. 2007, *A&A*, 471, 331
- Ehrenfreund, P., Gerakines, P. A., Shutte, W. A., van Hemert, M. C., & van Dishoeck, E. F. 1996, *A&A*, 312, 263
- Fulvio, D., Sivaraman, B., Baratta, G. A., Palumbo, M. E., & Mason, N. J. 2009, *Spectrochim. Acta A*, 72, 1007
- Gerakines, P. A., Bray, J. J., Davis, A., & Richey, C. R. 2005, *ApJ*, 620, 1140
- Gladman, B., Marsden, B. G., & VanLaerhoven, C. 2008, in *The Solar System Beyond Neptune* (Tucson: University of Arizona Press), 43
- Grundy, W. M., & Buie, M. W. 2001, *Icarus*, 153, 248
- Grundy, W. M. & Buie, M. W. 2002, *Icarus*, 157, 128
- Grundy, W. M., Buie, M. W., & Spencer, J. R. 2002, *AJ*, 124, 2273
- Hagen, W., Tielens, A. G. G. M., & Greenberg, J. M. 1983, *A&AS*, 51, 389
- Hudgins, D., Sandford, S. A., Allamandola, L. J., & Tielens, A. G. G. M. 1993, *ApJS*, 86, 713
- Jenniskens, P. & Blake, D. F. 1994, *Science*, 265, 753
- Jewitt, D. C., & Luu, J. 2004, *Nature*, 432, L731
- Johnson, R. E. 1990, in *Energetic charged-particle interactions with atmospheres and surfaces, X.* (Springer-Verlag Berlin Heidelberg New York).
- Kimmel, G. A., Stevenson, K. P., Dohnálek, Z., Smith, R. S., & Kay, B. D. 2001a, *J. Chem. Phys.*, 114, 5284
- Kimmel, G. A., Dohnálek, Z., Stevenson, K. P., Smith, R. S., & Kay, B. D. 2001b, *J. Chem. Phys.*, 114, 5295
- Licandro, J., Oliva, E., & Di Martino, M. 2001, *A&A*, 373, L29
- Licandro, J., Pinilla-Alonso, N., Pedani, M., et al. 2006a, *A&A*, 445, L35
- Licandro, J., Grundy, W. M., Pinilla-Alonso, N., & Leisy, P. 2006b, *A&A*, 458, L5
- Lellouch, E., Laureijs, R., Schmitt, B., et al. 2000, *Icarus*, 147, 220
- Leto, G., & Baratta, G. A. 2003, *A&A*, 397, 7
- Macleod, H. A. 1986, in *Thin-film optical filters*, ed. A. Hilger Ltd
- Mastrapa, R. M., Bernstein, M. P., Sandford, S. A., et al. 2008, *Icarus*, 197, 307
- McKinnon, W. B., Lunine, J. I., & Banfield, D. 1995, in *Neptune and Triton*, ed. Cruikshank (Tucson: Univ. of Arizona Press), 807
- Moore, M. H., & Hudson, R. L. 1992, *ApJ*, 401, 353
- Nelander, B. 1988, *J. Chem. Phys.*, 88, 5254
- Olkin, C. B., Young, E. F., Young, L. A., et al. 2007, *AJ*, 133, 420
- Owen, T. C., Roush, T. L., Cruikshank, D. P., et al. 1993, *Science*, 261, 745
- Palumbo, M. E. 1997, *J. Phys. Chem. A*, 101, 4298
- Palumbo, M. E. 2006, *A&A*, 453, 903
- Palumbo, M. E., & Strazzulla, G. 2003, *Canadian J. Phys.*, 81, 217
- Palumbo, M. E., Ferini, G., & Strazzulla, G. 2004, *Adv. Space Res.*, 33, 49
- Palumbo, M. E., Baratta, G. A., Collings, M. P., & McCoustra, M. R. S. 2006, *Phys. Chem. Chem. Phys.*, 8, 279
- Pinilla-Alonso, N., Brunetto, R., Licandro, J., et al. 2009 *A&A*, 496, 547
- Protopapa, S., Boehnhardt, H., Herbst, T. M., et al. 2008 *A&A*, 490, 365
- Quirico, E., & Schmitt, B. 1997, *Icarus*, 127, 354
- Quirico, E., Douté, S., Schmitt, B., et al. 1999, *Icarus*, 139, 159
- Raut, U., Famà, M., Loeffler, M. J., & Baragiola, R. A. 2008, *ApJ*, 687, 1070
- Reuter, D. C., Stern, S. A., Scherrer, J., et al. 2008, *Space Sci. Rev.*, 140, 129
- Rowland, B., Fisher, M., & Devlin, J. P. 1991, *J. Chem. Phys.*, 95, 1378
- Satorre, M. A., Palumbo, M. E., & Strazzulla, G. 2001, *J. Geophys. Res.*, 106, 33363
- Shaller, E. L., & Brown, M. E. 2007, *ApJ*, 670, L49
- Strazzulla, G., & Johnson, R. E. 1991, in *Comets in the post-Halley era*, 1, 243
- Strazzulla, G., Cooper, J. F., Christian, E. R., & Johnson, R. E. 2003, *C. R. Physique*, 4, 791
- Tegler, S. C., Grundy, W. M., Romanishin, W., et al. 2007, *ApJ*, 133, 526
- Tegler, S. C., Grundy, W. M., Vilas, F., et al. 2008, *Icarus*, 195, 844
- Tursi, A. J., & Nixon, E. R. 1970, *J. Chem. Phys.*, 52, 1521
- Westley, M. S., Baratta, G. A., & Baragiola, R. A. 1998, *J. Chem. Phys.*, 108, 3321
- Young, L. A., Stern, S. A., Weaver, H. A., et al. 2008, *Space Sci. Rev.*, 140, 93